Unsteady MHD Couette-Hartmann flow through a porous medium bounded by porous plates with Hall current, ion-slip and Coriolis effects

J. K. Singh [*][†], S. Ghousia Begum [‡]N. Joshi [§]

Abstract

Effects of Hall current, ion-slip and Coriolis force on unsteady MHD Couette-Hartmann flow of a viscous incompressible electrically conducting fluid through a porous medium bounded by porous plates in the presence of a uniform transverse magnetic field which is either fixed relative to the fluid or to the moving porous plate is investigated using Laplace transform technique. The expressions for the fluid velocity and shear stress at the moving porous plate are also derived. In order to analyze the physical significance and characteristic features of the problem, the graphs for velocity distribution and shear stress distribution at the moving porous plate are generated for different values of non-dimensional parameters. It is observed that the fluid velocity when magnetic field is fixed relative to the moving porous plate is always more than the fluid velocity when magnetic field is fixed relative to the fluid while the shear stress at the moving porous plate when magnetic field is fixed relative to the moving porous plate is always less than the shear stress at the moving porous plate when magnetic field is fixed relative to the fluid.

Keywords : Magnetic field; Hall current; Ion-slip; Coriolis force; Permeability and suction/injection.

1 Introduction

STudies made on magnetohydrodynamic (MHD) flows in a rotating environment has attracted many researchers during past several decades due to its occurrence in various natural phenomenon and technological situations. Investigation of interaction of electromagnetic force with Coriolis force is important because several geophysical, astrophysical and fluid engineering problems are governed by interaction of electromagnetic force and Coriolis force. MHD flow in a rotating system has practical application in MHD power generation, MHD Ekaman pumping and turbo machines. When an ionized fluid with low density is permeated by a strong magnetic field, the effect of Hall current may be significant (Sato [20]). Hall current is likely to be important in underground energy storage system, magneto meter, Hall effect sensors and spacecraft propulsion. It is observed that both the Coriolis force and Hall current induce secondary flow in the flow-field. Coriolis force and Hall current play vital role in determining the flow features of the MHD fluid flow problems. Taking into account these facts Chauhan and Agrawal [5], Ghosh [7],

[*]Corresponding author. s.jitendrak@yahoomail.com

[†]Department of Mathematics, V. S. K. University, Bellary-583105, INDIA.

[‡]Department of Mathematics, V. S. K. University, Bellary-583105, INDIA.

[§]Department of Mathematics, V. S. K. University, Bellary-583105, INDIA.

Ghosh and Pop [8, 9], Ghosh et al. [10], Guria and Jana [11], Jana and Datta [13], Jha and Apere [14, 15], Linga Raju and Ramana Rao [16], Nagy and Demendy [18], Ram *et al.* [19], Seth and Ansari [21], Seth and Ghosh [22], Seth and Singh [23], Seth et al. [24, 25], Singh and Kumar [27], Singh and Pathak [28], Sivaprasad *et al.* [29], Sulochana [31] and Takhar and Jha [33] studied combined effects of rotation and Hall current on MHD fluid flow problems in different conditions and configurations. In the case of very strong magnetic field, the diffusion velocity of ions may not be negligible. If we include the diffusion velocity of ions as well as that of electrons, we have the phenomenon of ion-slip (Cramer and Pai [6]). In such condition we include Hall current and ion-slip in the generalized Ohm's law for a moving conductor. Keeping this fact in mind Attia [2], Beg *et al.* [4], Jha and Apere [14, 15], Ram *et al.* [19], Soundalgekar *et al.*[30] and Takhar and Jha [33] investigated combined effects of Hall current and ion-slip on MHD flows considering different aspects of the problem.The governing equation for fluid motion through a porous medium is based on Darcy's law which determine the drag force exerted by porous medium (Ingham and Pop [12]). Study of MHD flows through a porous medium bounded by parallel plates is significant due to its application in the agricultural, bio-logical, geophysical and technological problems. Recently many researchers studied MHD flows of a viscous incompressible electrically conductiong fluid through a porous medium bounded by parallel plates in the presence of an applied magnetic field by considering various aspects of the problem. Mention may be made of the motivating research studies of Ahmed and Chamkha [1], Beg *et al.* [3, 4], Chauhan and Agrawal [5], Seth *et al.* [24], Singh *et al.* [26], Singh and Pathak [28] and Sulochana [31].

In the present study the effects of Hall Current, ion-slip and Coriolis force on unsteady MHD Couette-Hartmann flow of a viscous incom-pressible electrically conducting fluid through a porous medium bounded by porous plates in the presence of a uniform transverse magnetic field which is either fixed relative to the fluid or to the moving porous plate is analyzed. The fluid flow through the porous medium bounded by porous plates is induced due to an applied

pressure gradient acting along x-direction and due to time dependent movement of the upper plate along x-direction. Two particular cases of interest are considered i.e. (i) the case of small permeable regime and (ii) the case of pure fluid regime.
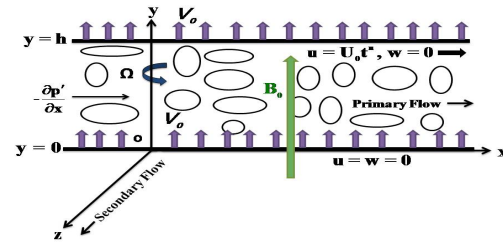

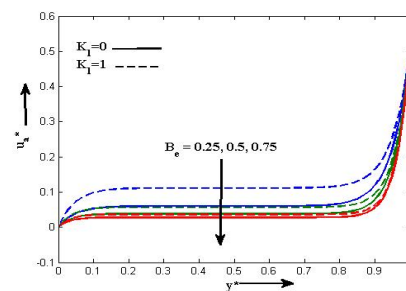**Figure 1:** Schematic diagram of the problem.

Figure 2: Velocity distribution in the primary flow direction when $B_i = 2.0$, $K^2 = 3$ and $N_t = 1.0$ in case of small permeable regime (i.e. $D_a = 0.01$).
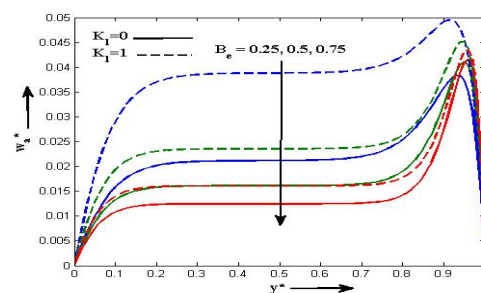

Figure 3: Velocity distribution in the secondary flow direction when $B_i = 2.0$, $K^2 = 3$ and $N_t = 1.0$ in case of small permeable regime (i.e. $D_a = 0.01$).

The fluid is assumed to be such that the magnetic Reynolds number $R_m = \mu_e \sigma U_0 h \ll 1$ (where μ_e, σ and h are, respectively, magnetic permeability, electrical conductivity and charac-teristic length) which corresponds to negligible induced magnetic field in comparison to ex-
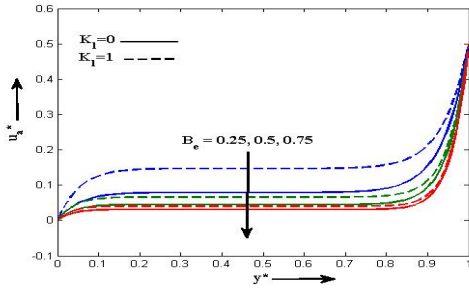
Figure 4: Velocity distribution in the primary flow direction when $B_i = 2.0$, $K^2 = 3$ and $N_t = 1.0$ in case of pure fluid regime (i.e. $D_a \to \infty$).

Figure 5: Velocity distribution in the secondary flow direction when $B_i = 2.0$, $K^2 = 3$ and $N_t = 1.0$ in case of pure fluid regime (i.e. $D_a \to \infty$).
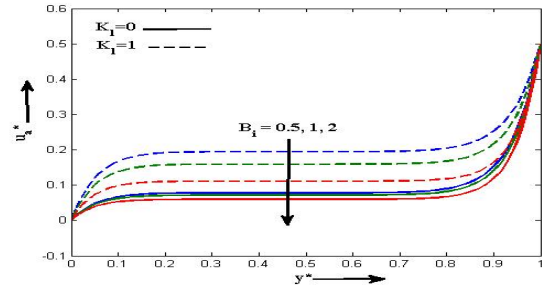

Figure 6: Velocity distribution in the primary flow direction when $B_e = 0.25$, $K^2 = 3$ and $N_t = 1.0$ in case of small permeable regime (i.e. $D_a = 0.01$).
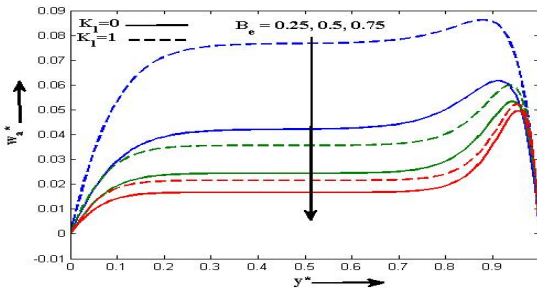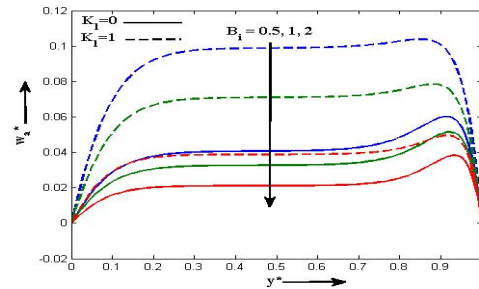

Figure 7: Velocity distribution in the secondary flow direction when $B_e = 0.25$, $K^2 = 3$ and $N_t = 1.0$ in case of small permeable regime (i.e. $D_a = 0.01$).

ternally applied magnetic field. Since there is no external applied or polarization voltages on the flow field, hence the induced electric field $\vec{E} = (0, 0, 0)$. Therefore the Maxwell's equations are uncoupled from the Navier-stokes equation (Cramer and Pai [6]). Since the plates are of infinite extent in x and z directions so all the fluid properties except pressure will depend on y and t only. In the essence of continuity equation the fluid velocity $\vec{q}$ can be assumed as $\vec{q} = (u, V_0, w)$.

The general equation of motion for hydromagnetic flow of a viscous incompressible electrically conducting fluid through a porous medium in a rotating system is given by

$$\begin{cases} \frac{\partial \vec{q}}{\partial t} + (\vec{q}.\nabla)\vec{q} + 2\vec{\Omega} \times \vec{q} = -\frac{1}{\rho}\nabla p\prime + \\ \nu \ \nabla^2 \vec{q} + \frac{1}{\rho}\vec{J} \times \vec{B} - \frac{\nu \vec{q}}{k}, \end{cases} \quad (1.1)$$

where $\rho, p\prime, \upsilon, \vec{J}$ and k are, respectively, fluid density, modified pressure, kinematic coefficient of viscosity, current density and permeability of the porous medium.

In the presence of a strong applied magnetic field B_0 the generalized Ohm's law for a moving conductor taking Hall current and ion-slip into account is given in the following form (Sutton and Sherman [32])

$$\begin{cases} \vec{J} = \sigma[\vec{E} + (\vec{q} \times \vec{B})] - \frac{B_e}{B_0}(\vec{J} \times \vec{B}) \\ +\frac{B_e B_i}{B_0^2}(\vec{J} \times \vec{B}) \times \vec{B}, \end{cases} \quad (1.2)$$

where B_e and B_i are, respectively, Hall current and ion-slip parameters.

In the essence of above assumptions, the equations governing the flow are

$$\begin{cases} \frac{\partial u}{\partial t} + V_0 \frac{\partial u}{\partial y} + 2\Omega w = -\frac{1}{\rho}\frac{\partial p\prime}{\partial x} + \upsilon\frac{\partial^2 u}{\partial y^2} \\ -\frac{\sigma B_0^2}{\rho}\left[\frac{u(1+B_e B_i)+wB_e}{(1+B_e B_i)^2+B_e^2}\right] - \frac{\upsilon u}{k}, \end{cases} \quad (1.3)$$

$$0 = -\frac{1}{\rho}\frac{\partial p\prime}{\partial y}, \quad (1.4)$$

$$\begin{cases} \frac{\partial w}{\partial t} + V_0 \frac{\partial w}{\partial y} - 2\Omega u = \upsilon\frac{\partial^2 w}{\partial y^2} \\ -\frac{\sigma B_0^2}{\rho}\left[\frac{w(1+B_e B_i)-uB_e}{(1+B_e B_i)^2+B_e^2}\right] - \frac{\upsilon w}{k}. \end{cases} \quad (1.5)$$
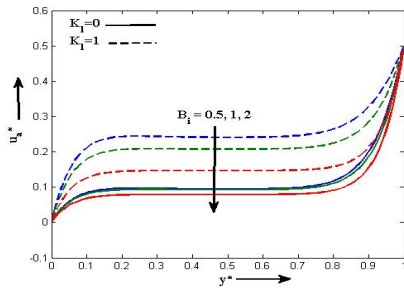
Figure 8: Velocity distribution in the primary flow direction when $B_e = 0.25$, $K^2 = 3$ and $N_t = 1.0$ in case of pure fluid regime (i.e. $D_a \to \infty$).

Figure 9: Velocity distribution in the secondary flow direction when $B_e = 0.25$, $K^2 = 3$ and $N_t = 1.0$ in case of pure fluid regime (i.e. $D_a \to \infty$).

Eq. (1.4) shows that modified pressure $p\prime$ is constant along y-axis i.e. along the axis of rotation. Since there is a net cross flow along z-axis so the pressure gradient term is absent in Eq. (1.5).

The initial and boundary conditions relevant to the problem are

$$t \le 0 : u = w = 0 \quad \forall y, \qquad (1.6)$$

$$t > 0 : u = w = 0 \quad \text{at} \quad y = 0, \qquad (1.7)$$

$$t > 0 : u = U_0 t^n, \quad w = 0 \quad \text{at} \quad y = h. \qquad (1.8)$$

Eq. (1.3) is valid when the magnetic field is fixed relative to the fluid. On the other hand when the magnetic lines of force are fixed related to the moving porous plate i.e. the magnetic lines of force are also moving with the velocity $U_0 t^n$, we must account for the relating motion, then Eq. (1.3) can be replaced by the following equation

$$\begin{cases} \frac{\partial u}{\partial t} + V_0 \frac{\partial u}{\partial y} + 2\Omega w = -\frac{1}{\rho}\frac{\partial p\prime}{\partial x} + \upsilon \frac{\partial^2 u}{\partial y^2} \\ -\frac{\sigma B_0^2}{\rho}\left[\frac{u(1+B_e B_i)+wB_e-U_0 t^n}{(1+B_e B_i)^2+B_e^2}\right] - \frac{\upsilon u}{k}. \end{cases} \qquad (1.9)$$
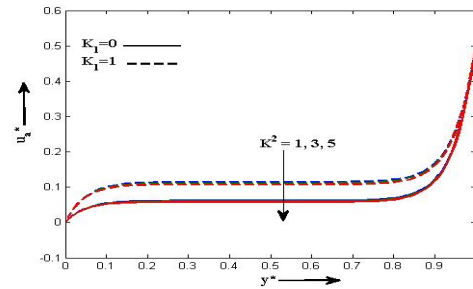
Eq. (1.3) and (1.9) can be combinedly repre-

Figure 10: Velocity distribution in the primary flow direction when $B_e = 0.25$, $B_i = 2.0$ and $N_t = 1.0$ in case of small permeable regime (i.e. $D_a = 0.01$).
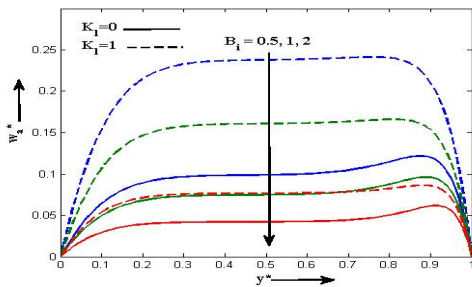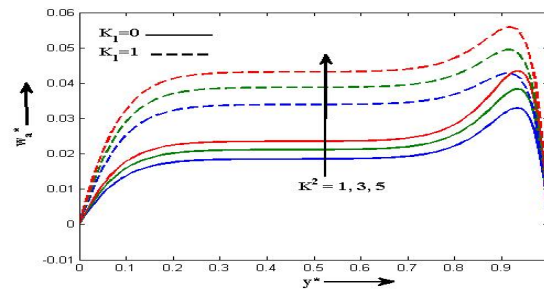

Figure 11: Velocity distribution in the secondary flow direction when $B_e = 0.25$, $B_i = 2.0$ and $N_t = 1.0$ in case of small permeable regime (i.e. $D_a = 0.01$).

sented by a single equation

$$\begin{cases} \frac{\partial u}{\partial t} + V_0 \frac{\partial u}{\partial y} + 2\Omega w = -\frac{1}{\rho}\frac{\partial p\prime}{\partial x} + \upsilon \frac{\partial^2 u}{\partial y^2} \\ -\frac{\sigma B_0^2}{\rho}\left[\frac{u(1+B_e B_i)+wB_e-K_1 U_0 t^n}{(1+B_e B_i)^2+B_e^2}\right] \\ -\frac{\upsilon u}{k}, \end{cases} \qquad (1.10)$$

where

$$K_1 = \begin{cases} 0 & \text{when } B_0 \text{ is fixed relative to the} \\ & \text{fluid} \\ 1 & \text{when } B_0 \text{ is fixed relative to the} \\ & \text{moving porous plate.} \end{cases}$$

The mathematical model of the present physical problem is represented by Eqs. (1.5) and (1.10) with initial and boundary conditions (1.6) to (1.8). Now it is essential to find the solution of Eqs. (1.5) and (1.10) with the initial and boundary conditions (1.6) to (1.8).

2   Solution of the Problem

The flow described by Eqs. (1.5) and (1.10) is the general representation of the fluid velocity
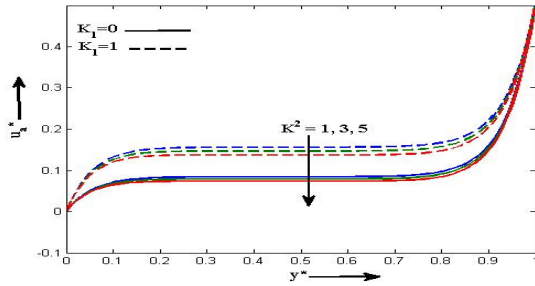
Figure 12: Velocity distribution in the primary flow direction when $B_e = 0.25$, $B_i = 2.0$ and $N_t = 1.0$ in case of pure fluid regime (i.e. $D_a \to \infty$).
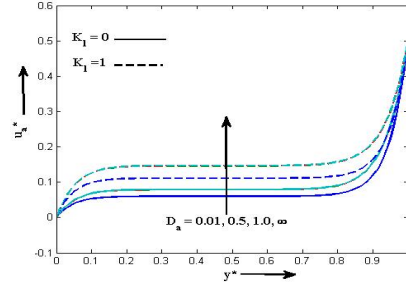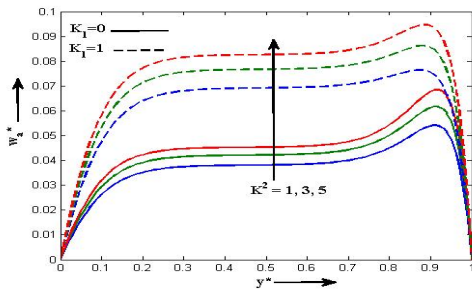

Figure 13: Velocity distribution in the secondary flow direction when $B_e = 0.25$, $B_i = 2.0$ and $N_t = 1.0$ in case of pure fluid regime (i.e. $D_a \to \infty$).

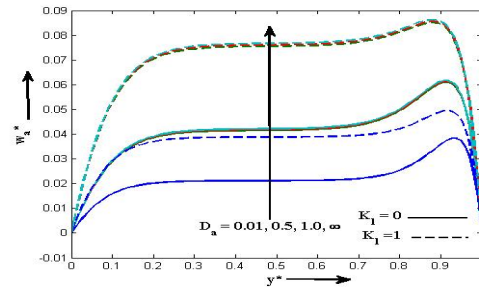**Figure 14:** Velocity distribution in the primary flow direction when $B_e = 0.25$, $B_i = 2.0$, $K^2 = 3$ and $N_t = 1.0$.

Figure 15: Velocity distribution in the secondary flow direction when $B_e = 0.25$, $B_i = 2.0$, $K^2 = 3$ and $N_t = 1.0$.

for the Couette-Hartmann flow through a porous medium bounded by infinite porous plates due to movement of the upper plate and applied pressure gradient. In order to analyze the specific flow pattern we have considered the case when $n = 1$ which corresponds to the uniformly accelerated motion. Combining Eqs. (1.5) and (1.10) by putting $n = 1$, the governing equation in compact form, become

$$
\begin{cases}
\frac{\partial q_1}{\partial t} + V_0 \frac{\partial q_1}{\partial y} - 2i\Omega q_1 = \\
-\frac{1}{\rho} \frac{\partial p\prime}{\partial x} + \upsilon \frac{\partial^2 q_1}{\partial y^2} \\
-\frac{\sigma B_0^2}{\rho} \left[\frac{\{(1+B_e B_i) - iB_e\}q_1 - K_1 U_0 t}{(1+B_e B_i)^2 + B_e^2} \right] \\
-\frac{\upsilon q_1}{k},
\end{cases} \quad (2.11)
$$

where $q_1 = u + iw$.

The initial and boundary conditions in compact form after taking $n = 1$, are given by

$$
t \leq 0 : q_1 = 0 \quad \forall y \quad , \qquad (2.12)
$$

$$
t > 0 : q_1 = 0 \quad \text{at} \quad y = 0, \qquad (2.13)
$$

$$
t > 0 : q_1 = U_0 t, \quad \text{at} \quad y = h. \qquad (2.14)
$$

Introducing following non-dimensional quantities

$$
x^* = \frac{x}{h}, \quad y^* = \frac{y}{h}, \quad q_1^* = \frac{q_1}{U_0},
$$

$$
p^* = \frac{p\prime}{\rho U_0^2} \quad \text{and} \quad t^* = \frac{tU_0}{h}.
$$

Eq. (2.11) in non-dimensional form become

$$
\begin{cases}
\frac{\partial q_1^*}{\partial t^*} + N_t \frac{\partial q_1^*}{\partial y^*} - 2iK^2 q_1^* = R + \frac{1}{R_e} \frac{\partial^2 q_1^*}{\partial y^{*2}} \\
-\frac{H_a^2}{R_e} \left[\frac{\{(1+B_e B_i) - iB_e\}q_1^* - K_1 R_1 t^*}{(1+B_e B_i)^2 + B_e^2} \right] \\
-\frac{q_1^*}{D_a R_e},
\end{cases} \quad (2.15)
$$

and the initial and boundary conditions assumes the following non-dimensional form

$$
t^* \leq 0 : q_1^* = 0 \quad \forall y^*, \qquad (2.16)
$$

$$
t^* > 0 : q_1^* = 0 \quad \text{at} \quad y^* = 0, \qquad (2.17)
$$

$$
t^* > 0 : q_1^* = R_1 t^* \quad \text{at} \quad y^* = 1. \qquad (2.18)
$$

where $N_t = V_0/U_0$ is suction/injection parameter ($N_t > 0$ for suction and $N_t < 0$ for injection) which represents the mass of fluid passing into the porous channel via the stationary plate
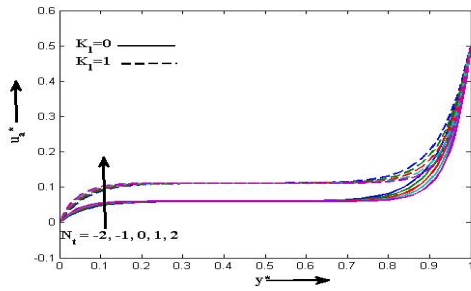
Figure 16: Velocity distribution in the primary flow direction when $B_e = 0.25$, $B_i = 2.0$ and $K^2 = 3$ in case of small permeable regime (i.e. $D_a = 0.01$).
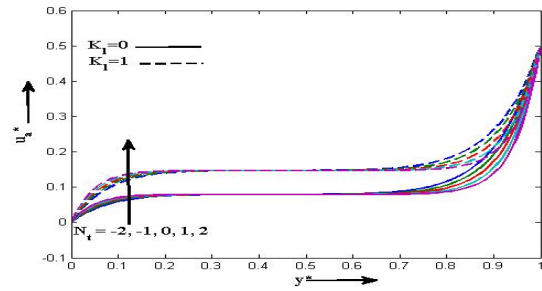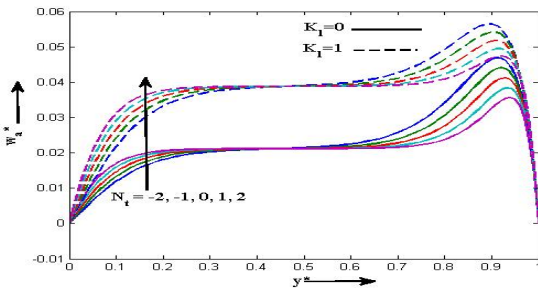

Figure 17: Velocity distribution in the secondary flow direction when $B_e = 0.25$, $B_i = 2.0$ and $K^2 = 3$ in case of small permeable regime (i.e. $D_a = 0.01$).
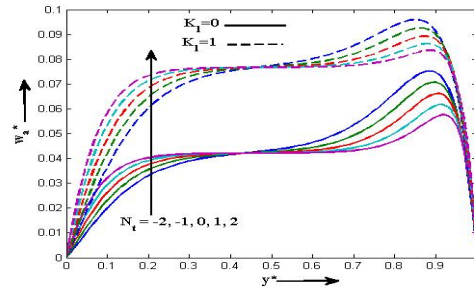

Figure 18: Velocity distribution in the primary flow direction when $B_e = 0.25$, $B_i = 2.0$ and $K^2 = 3$ in case of pure fluid regime (i.e. $D_a \to \infty$).

Figure 19: Velocity distribution in the secondary flow direction when $B_e = 0.25$, $B_i = 2.0$ and $K^2 = 3$ in case of pure fluid regime (i.e. $D_a \to \infty$).

and exiting via the moving plate, $K^2 = \Omega h/U_0$ is rotation parameter which represents the relative strength of Coriolis force to the inertial force, $R = -\partial p^*/\partial x^*$ is modified pressure gradient, $R_e = hU_0/\upsilon$ is Reynolds number which represents the relative strength of inertial force to the viscous force, $H_a^2 = \sigma B_0^2 h^2/\rho\upsilon$ is square of Hartmann number (magnetic parameter) which represents the relative strength of magnetic force to the viscous force, $D_a = k/h^2$ is Darcy number (permeability parameter) which represents the relative permeability of porous channel and $R_1 = h/U_0$ is a constant.

The analytical solution of Eq. (2.15) subject to the initial and boundary conditions (2.16) to (2.18) is obtained by Laplace transform technique. Define the Laplace transform variable

$$\overline{q_1^*}(y^*, s) = \int_0^\infty e^{-st^*} q_1^*(y^*, t^*) \mathrm{d}t^*$$

where s is Laplace transform parameter, $s > 0$ and then taking Laplace transform of Eq. (2.15) and using initial condition (2.16), Eq. (2.15)

transform to the following equation

$$
\begin{cases}
\dfrac{\mathrm{d}^2 \overline{q_1^*}}{\mathrm{d}y^{*2}} - N_t R_e \dfrac{\mathrm{d}\overline{q_1^*}}{\mathrm{d}y^*} - R_e \left[s + \dfrac{1}{D_a R_e} \right. \\[2mm]
\left. + \dfrac{H_a^2(1 + B_e B_i)}{R_e((1 + B_e B_i)^2 + B_e^2)} \right. \\[2mm]
\left. -i \left\{ 2K^2 + \dfrac{H_a^2 B_e}{R_e((1 + B_e B_i)^2 + B_e^2)} \right\} \right] \overline{q_1^*} \\[2mm]
= -\dfrac{H_a^2 R_1 K_1}{s^2((1 + B_e B_i)^2 + B_e^2)} - \dfrac{R R_e}{s}.
\end{cases}
\tag{2.19}
$$

The boundary conditions (2.17) and (2.18) after taking Laplace transform, transform to the equations

$$\overline{q_1^*} = 0 \quad \text{at} \quad y^* = 0, \tag{2.20}$$

$$\overline{q_1^*} = \frac{R_1}{s^2} \quad \text{at} \quad y^* = 1. \tag{2.21}$$

The solution of the Eq. (2.19) subject to the boundary conditions (2.20) and (2.21) is
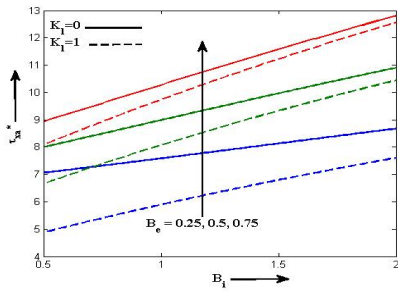
Figure 20: Shear stress distribution in the primary flow direction when $K^2 = 3$ and $N_t = 1.0$ in case of small permeable regime (i.e. $D_a = 0.01$).
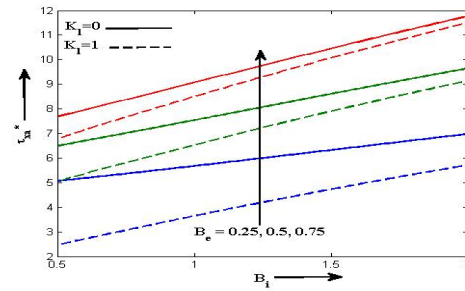

Figure 22: Shear stress distribution in the primary flow direction when $K^2 = 3$ and $N_t = 1.0$ in case of pure fluid regime (i.e. $D_a \to \infty$).
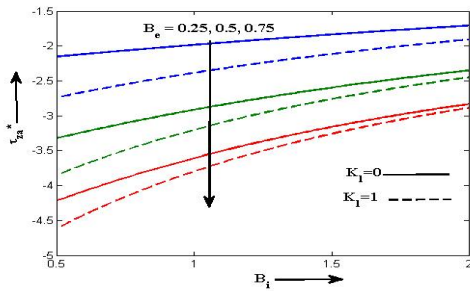

Figure 21: Shear stress distribution in the secondary flow direction when $K^2 = 3$ and $N_t = 1.0$ in case of small permeable regime (i.e. $D_a = 0.01$).
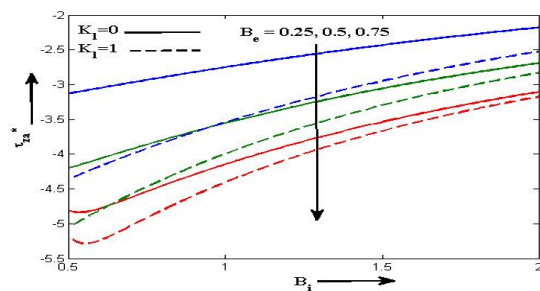

Figure 23: Shear stress distribution in the secondary flow direction when $K^2 = 3$ and $N_t = 1.0$ in case of pure fluid regime (i.e. $D_a \to \infty$).

$$
\begin{cases}
\overline{q_a^*} = \frac{K_1 X_1}{s^2 X_5} - \left(\frac{K_1 X_1 - X_5 R^*}{X_5^2} \right) \\
\times \left[\frac{1}{s} - \frac{1}{s + X_5} \right] \\
+ \sum_{n=0}^{\infty} \left[\left(\frac{e^{-a\lambda_1} - e^{-b\lambda_1}}{s^2} \right) \right. \\
- (-1)^n \left[\frac{K_1 X_1}{X_5} \left(\frac{e^{-c\lambda_1} + e^{-d\lambda_1}}{s^2} \right) \right. \\
- \left(\frac{K_1 X_1 - X_5 R^*}{X_5^2} \right) \left\{ \left(\frac{e^{-c\lambda_1} + e^{-d\lambda_1}}{s} \right) \right. \\
\left. \left. \left. - \left(\frac{e^{-c\lambda_1} + e^{-d\lambda_1}}{s + X_5} \right) \right\} \right] \right],
\end{cases} \quad (2.22)
$$

where

$$a = 2n + 1 - y^*, b = 2n + 1 + y^*,$$

$$c = n + y^*, d = n + 1 - y^*,$$

$$X_1 = \frac{H_a^2}{R_e \left((1 + B_i B_e)^2 + B_e^2 \right)}, X_2 = B_e X_1,$$

$$X_3 = \frac{1}{D_a R_e} + (X_1 + B_i X_2),$$

$$X_4 = 2K^2 + X_2, X_5 = X_3 - iX_4,$$

$$\alpha, \beta = \frac{1}{\sqrt{2}} \left[\left\{ \left(\frac{N_t^2 R_e}{4} + X_3 \right)^2 + X_4^2 \right\}^{\frac{1}{2}} \right.$$

$$\pm \left(\frac{N_t^2 R_e}{4} + X_3 \right) \right]^{\frac{1}{2}},$$

$$q_a^* = \frac{q_1^*}{R_1} = u_a^* + iw_a^*, \quad R^* = \frac{R}{R_1},$$

$$P = \alpha - i\beta,$$

$$\lambda_1 = (N_t R_e / 2) + \sqrt{R_e}\sqrt{s + P^2}.$$

Using following Fourier-Mellin inversion integral formula to invert Eq. (2.22)

$$
\begin{cases}
L^{-1} \left[\frac{e^{-y_1(s+g)^{1/2}}}{s^{N+1}} \right] = F(y_1, t^*, g, N) \\
= \frac{1}{2\pi i} \int_{Br_2} \frac{e^{st^*} e^{-y_1(s+g)^{1/2}}}{s^{N+1}} \mathrm{d}s,
\end{cases} \quad (2.23)
$$

$$
\begin{cases}
L^{-1} \left[\frac{e^{-y_1(s+g)^{1/2}}}{(s-a_1)^{N+1}} \right] = G(y_1, t^*, g, N) \\
= \frac{1}{2\pi i} \int_{Br_2} \frac{e^{st^*} e^{-y_1(s+g)^{1/2}}}{(s-a_1)^{N+1}} \mathrm{d}s,
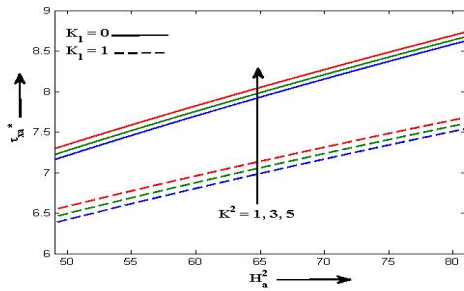\end{cases} \quad (2.24)
$$

Figure 24: Shear stress distribution in the primary flow direction when $B_e = 0.25, B_i = 2.0$ and $N_t = 1.0$ in case of small permeable regime (i.e. $D_a = 0.01$).
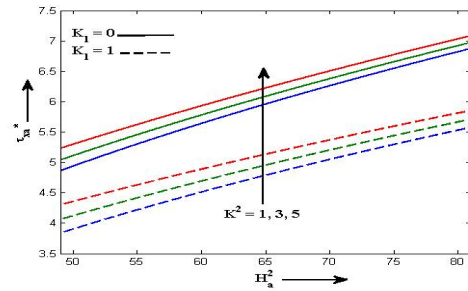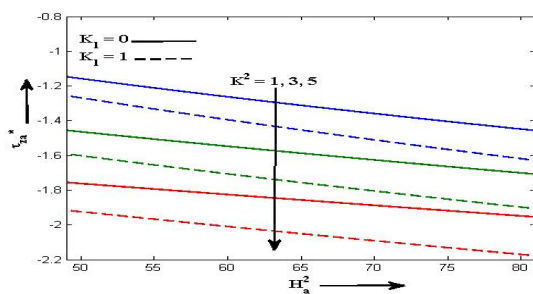

Figure 25: Shear stress distribution in the secondary flow direction when $B_e = 0.25, B_i = 2.0$ and $N_t = 1.0$ in case of small permeable regime (i.e. $D_a = 0.01$).

Figure 26: Shear stress distribution in the primary flow direction when $B_e = 0.25, B_i = 2.0$ and $N_t = 1.0$ in case of pure fluid regime (i.e. $D_a \to \infty$).
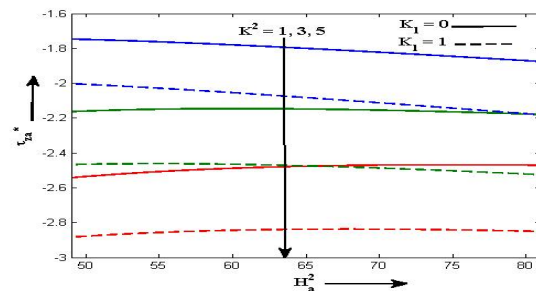
Figure 27: Shear stress distribution in the secondary flow direction when $B_e = 0.25, B_i = 2.0$ and $N_t = 1.0$ in case of pure fluid regime (i.e. $D_a \to \infty$).

and

$$\begin{cases} F(y_1, t^*, g, N) \\ = \frac{\mathrm{d}}{dg} \left[F(y_1, t^*, g, N-1) \right] \\ + t^* F(y_1, t^*, g, N-1), \end{cases} \quad (2.25)$$

where Br_2 is Bromwich path defined by McLachlan [17].
When $N = 0$, from Eqs. (2.23) and (2.24), we have

$$\begin{cases} F(y_1, t^*, g, 0) = \frac{1}{2} \Bigg\{ e^{y_1 \sqrt{g}} \\ \times erfc \left(\frac{y_1}{2\sqrt{t^*}} + \sqrt{gt^*} \right) + e^{-y_1 \sqrt{g}} \\ \times erfc \left(\frac{y_1}{2\sqrt{t^*}} - \sqrt{gt^*} \right) \Bigg\}, \end{cases} \quad (2.26)$$

$$\begin{cases} G(y_1, t^*, g, 0) = \frac{e^{a_1 t^*}}{2} \Bigg\{ e^{y_1 \sqrt{g_1}} \\ \times erfc \left(\frac{y_1}{2\sqrt{t^*}} + \sqrt{g_1 t^*} \right) + e^{-y_1 \sqrt{g_1}} \\ \times erfc \left(\frac{y_1}{2\sqrt{t^*}} - \sqrt{g_1 t^*} \right) \Bigg\}, \end{cases} \quad (2.27)$$

where $g_1 = a_1 + g$.

When $N = 1$, from Eqs. (2.25) and (2.26), we obtain

$$\begin{cases} F(y_1, t^*, g, 1) = \frac{1}{4\sqrt{g}} \Bigg\{ (2t^* \sqrt{g} + y_1) \\ \times e^{y_1 \sqrt{g}} erfc \left(\frac{y_1}{2\sqrt{t^*}} + \sqrt{gt^*} \right) \\ + (2t^* \sqrt{g} - y_1) \\ \times e^{-y_1 \sqrt{g}} erfc \left(\frac{y_1}{2\sqrt{t^*}} - \sqrt{gt^*} \right) \Bigg\}. \end{cases} \quad (2.28)$$

After inverting Eq. (2.22), the solution for fluid

velocity are presented in the following form

$$
\begin{cases}
q_a^* = \frac{X_1 K_1 t^*}{X_5} - \left[\frac{X_1 K_1 - X_5 R^*}{X_5^2} \right] \\
\times \left(1 - e^{-X_5 t^*} \right) + \frac{1}{2} \sum_{n=0}^{\infty} \left[\left\{ A_1 e^{-aP_1} \right. \right. \\
\times erfc \left(\frac{a}{2}\sqrt{\frac{R_e}{t^*}} - P\sqrt{t^*} \right) \\
+ A_2 e^{-aP_2} erfc \left(\frac{a}{2}\sqrt{\frac{R_e}{t^*}} + P\sqrt{t^*} \right) \right\} \\
- \left\{ B_1 e^{-bP_1} erfc \left(\frac{b}{2}\sqrt{\frac{R_e}{t^*}} - P\sqrt{t^*} \right) \right. \\
+ B_2 e^{-bP_2} erfc \left(\frac{b}{2}\sqrt{\frac{R_e}{t^*}} + P\sqrt{t^*} \right) \right\} \\
- (-1)^n \left\{ \frac{X_1 K_1}{X_5} \left\{ C_1 e^{-cP_1} \right. \right. \\
\times erfc \left(\frac{c}{2}\sqrt{\frac{R_e}{t^*}} - P\sqrt{t^*} \right) \\
+ C_2 e^{-cP_2} erfc \left(\frac{c}{2}\sqrt{\frac{R_e}{t^*}} + P\sqrt{t^*} \right) \\
+ D_1 e^{-dP_1} erfc \left(\frac{d}{2}\sqrt{\frac{R_e}{t^*}} - P\sqrt{t^*} \right) \\
+ D_2 e^{-dP_2} erfc \left(\frac{d}{2}\sqrt{\frac{R_e}{t^*}} + P\sqrt{t^*} \right) \right\} \\
- \left(\frac{X_1 K_1 - X_5 R^*}{X_5^2} \right) \left\{ e^{-cP_1} \right. \\
\times erfc \left(\frac{c}{2}\sqrt{\frac{R_e}{t^*}} - P\sqrt{t^*} \right) \\
+ e^{-cP_2} erfc \left(\frac{c}{2}\sqrt{\frac{R_e}{t^*}} + P\sqrt{t^*} \right) \\
+ e^{-dP_1} erfc \left(\frac{d}{2}\sqrt{\frac{R_e}{t^*}} - P\sqrt{t^*} \right) \\
+ e^{-dP_2} erfc \left(\frac{d}{2}\sqrt{\frac{R_e}{t^*}} + P\sqrt{t^*} \right) \\
- e^{-X_5 t^*} \left\{ e^{-cN_t R_e} \right. \\
\times erfc \left(\frac{c}{2}\sqrt{\frac{R_e}{t^*}} - \frac{N_t \sqrt{R_e t^*}}{2} \right) \\
+ erfc \left(\frac{c}{2}\sqrt{\frac{R_e}{t^*}} + \frac{N_t \sqrt{R_e t^*}}{2} \right) \\
+ e^{-dN_t R_e} erfc \left(\frac{d}{2}\sqrt{\frac{R_e}{t^*}} - \frac{N_t \sqrt{R_e t^*}}{2} \right) \\
+ erfc \left(\frac{d}{2}\sqrt{\frac{R_e}{t^*}} + \frac{N_t \sqrt{R_e t^*}}{2} \right) \right\}\right\}\right\}\right],
\end{cases}
$$

(2.29)

where

$$
A_1 = \left(t^* - \frac{a\sqrt{R_e}}{2P} \right), \quad A_2 = \left(t^* + \frac{a\sqrt{R_e}}{2P} \right),
$$

$$
B_1 = \left(t^* - \frac{b\sqrt{R_e}}{2P} \right), \quad B_2 = \left(t^* + \frac{b\sqrt{R_e}}{2P} \right),
$$

$$
C_1 = \left(t^* - \frac{c\sqrt{R_e}}{2P} \right), \quad C_2 = \left(t^* + \frac{c\sqrt{R_e}}{2P} \right),
$$

$$
D_1 = \left(t^* - \frac{d\sqrt{R_e}}{2P} \right), \quad D_2 = \left(t^* + \frac{d\sqrt{R_e}}{2P} \right),
$$

$$
P_1 = \left(\frac{N_t R_e}{2} + P\sqrt{R_e} \right),
$$

$$
P_2 = \left(\frac{N_t R_e}{2} - P\sqrt{R_e} \right).
$$

The fluid velocity when magnetic field is fixed relative to the fluid is obtained by putting $K_1 = 0$ in Eq. (2.29) while the fluid velocity when magnetic field is fixed relative to the moving porous plate is found by putting $K_1 = 1$ in Eq. (2.29).

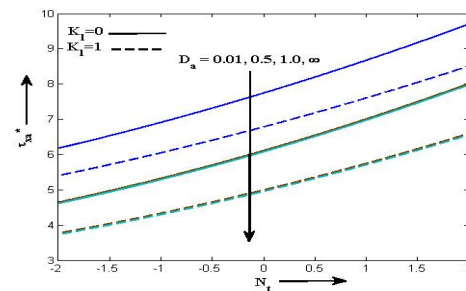**Figure 28:** Shear stress distribution in the primary flow direction when $B_e = 0.25$, $B_i = 2.0$ and $K^2 = 3$.
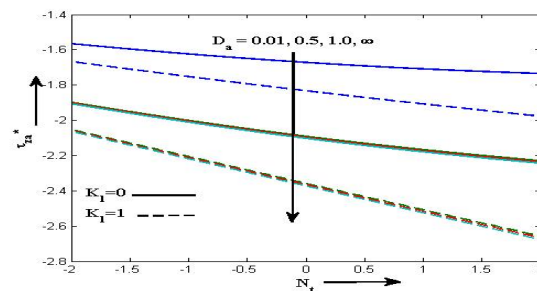

Figure 29: Shear stress distribution in the secondary flow direction when $B_e = 0.25$, $B_i = 2.0$ and $K^2 = 3$.

3   Shear Stress at the Moving Porous Plate

The non-dimensional shear stress in the primary flow direction τ_{xa}^* and the non-dimensional shear stress in the secondary flow direction τ_{za}^* at the moving porous plate when magnetic field is either fixed relative to the fluid ($K_1 = 0$) or to the moving porous plate ($K_1 = 1$) are given by

$$
\begin{aligned}
\tau_{xa}^* + i\tau_{za}^* = \frac{\sqrt{R_e}}{2} \sum_{n=0}^{\infty} \Bigg[\Bigg\{ A_1' e^{-a'P_1} \\
\times erfc\left(\frac{a'}{2}\sqrt{\frac{R_e}{t^*}} - P\sqrt{t^*}\right) \\
- A_2' e^{-a'P_2} erfc\left(\frac{a'}{2}\sqrt{\frac{R_e}{t^*}} + P\sqrt{t^*}\right) \Bigg\} \\
- \Bigg\{ B_1' e^{-b'P_1} erfc\left(\frac{b'}{2}\sqrt{\frac{R_e}{t^*}} - P\sqrt{t^*}\right) \\
- B_2' e^{-b'P_2} erfc\left(\frac{b'}{2}\sqrt{\frac{R_e}{t^*}} + P\sqrt{t^*}\right) \Bigg\} \\
+ 2\sqrt{\frac{t^*}{\pi}} A - (-1)^{n+1} \Bigg\{ \frac{X_1 K_1}{X_5} \Bigg\{ \Bigg\{ C_1' e^{-c'P_1} \\
\times erfc\left(\frac{c'}{2}\sqrt{\frac{R_e}{t^*}} - P\sqrt{t^*}\right) \\
- C_2' e^{-c'P_2} erfc\left(\frac{c'}{2}\sqrt{\frac{R_e}{t^*}} + P\sqrt{t^*}\right) \Bigg\} \\
- \Bigg\{ D_1' e^{-d'P_1} erfc\left(\frac{d'}{2}\sqrt{\frac{R_e}{t^*}} - P\sqrt{t^*}\right) \\
- D_2' e^{-d'P_2} erfc\left(\frac{d'}{2}\sqrt{\frac{R_e}{t^*}} + P\sqrt{t^*}\right) \Bigg\} \\
+ 2\sqrt{\frac{t^*}{\pi}} B \Bigg\} - \left[\frac{X_1 K_1 - X_5 R^*}{X_5^2}\right] \\
\times \Bigg\{ \Bigg\{ P_1' e^{-c'P_1} erfc\left(\frac{c'}{2}\sqrt{\frac{R_e}{t^*}} - P\sqrt{t^*}\right) \\
+ P_2' e^{-c'P_2} erfc\left(\frac{c'}{2}\sqrt{\frac{R_e}{t^*}} + P\sqrt{t^*}\right) \Bigg\} \\
- \Bigg\{ P_1' e^{-d'P_1} erfc\left(\frac{d'}{2}\sqrt{\frac{R_e}{t^*}} - P\sqrt{t^*}\right) \\
+ P_2' e^{-d'P_2} erfc\left(\frac{d'}{2}\sqrt{\frac{R_e}{t^*}} + P\sqrt{t^*}\right) \Bigg\} \\
+ \frac{2}{\sqrt{\pi t^*}} B + e^{-X_5 t^*} \Bigg\{ N_t \sqrt{R_e} \Bigg\{ e^{-c'N_t R_e}
\end{aligned}
$$

$$
\begin{aligned}
\times erfc\left(\frac{c'}{2}\sqrt{\frac{R_e}{t^*}} - \frac{N_t\sqrt{R_e t^*}}{2}\right) \\
- e^{-d'N_t R_e} erfc\left(\frac{d'}{2}\sqrt{\frac{R_e}{t^*}} - \frac{N_t\sqrt{R_e t^*}}{2}\right) \Bigg\} \\
+ \frac{2}{\sqrt{\pi t^*}} C \Bigg\} \Bigg\} \Bigg\} \Bigg],
\end{aligned}
$$

(3.30)

where

$$a' = 2n, \quad b' = 2(n+1), \quad c' = n+1,$$

$$d' = n, \quad P_1' = \left(\frac{N_t\sqrt{Re}}{2} + P\right),$$

$$P_2' = \left(\frac{N_t\sqrt{Re}}{2} - P\right),$$

$$A = \Bigg\{ e^{-\left(\frac{a'^2 Re}{4t^*} + \frac{a' N_t Re}{2} + P^2 t^*\right)} \\
- e^{-\left(\frac{b'^2 Re}{4t^*} + \frac{b' N_t Re}{2} + P^2 t^*\right)} \Bigg\},$$

$$B = \Bigg\{ e^{-\left(\frac{c'^2 Re}{4t^*} + \frac{c' N_t Re}{2} + P^2 t^*\right)} \\
- e^{-\left(\frac{d'^2 Re}{4t^*} + \frac{d' N_t Re}{2} + P^2 t^*\right)} \Bigg\},$$

$$C = \Bigg\{ e^{-\left(\frac{c'^2 Re}{4t^*} + \frac{c' N_t Re}{2} + \frac{N_t^2 Re t^*}{4}\right)} \\
- e^{-\left(\frac{d'^2 Re}{4t^*} + \frac{d' N_t Re}{2} + \frac{N_t^2 Re t^*}{4}\right)} \Bigg\},$$

$$A_1' = \frac{1}{2P} + \left(t^* - \frac{a'\sqrt{R_e}}{2P}\right) P_1',$$

$$A_2' = \frac{1}{2P} - \left(t^* + \frac{a'\sqrt{R_e}}{2P}\right) P_2',$$

$$B_1' = \frac{1}{2P} + \left(t^* - \frac{b'\sqrt{R_e}}{2P}\right) P_1',$$

$$B_2' = \frac{1}{2P} - \left(t^* + \frac{b'\sqrt{R_e}}{2P}\right) P_2',$$

$$C_1' = \frac{1}{2P} + \left(t^* - \frac{c'\sqrt{R_e}}{2P}\right) P_1',$$

$$C_2' = \frac{1}{2P} - \left(t^* + \frac{c'\sqrt{R_e}}{2P}\right) P_2',$$

$$D_1' = \frac{1}{2P} + \left(t^* - \frac{d'\sqrt{R_e}}{2P}\right) P_1',$$

$$D_2' = \frac{1}{2P} - \left(t^* + \frac{d'\sqrt{R_e}}{2P}\right) P_2'.$$

4   Results and Analysis

In order to observe physical insight into this fluid flow problem the graphs for velocity distribution and shear stress distribution at the moving porous plate are computed and generated for various values of different non-dimensional parameters taking $H_a^2 = 81, t^* = 0.5, R = 5$ and $R_e = 4$. The values of non-dimensional parameters corresponding to each figure are included in the caption of the figure and there inside the figure. Figs. 2 to 5 show the influence of Hall current parameter B_e on the fluid velocity in the primary and secondary flow directions. Figs. 2 and 4 display that in case of both the small permeable regime ($D_a = 0.01$) and pure fluid regime ($D_a \rightarrow \infty$), fluid velocity in the primary flow direction u_a^* decreases on increasing Hall current parameter B_e when magnetic field is either fixed relative to the fluid ($K_1 = 0$) or to the moving porous plate ($K_1 = 1$). Figs. 3 and 5 represent that in case of both the small permeable regime ($D_a = 0.01$) and pure fluid regime ($D_a \rightarrow \infty$), fluid velocity in the secondary flow direction w_a^* decreases on increasing Hall current parameter B_e in most part of the channel whereas it increases on increasing Hall current parameter B_e in the vicinity of the moving porous plate when magnetic field is either fixed relative to the fluid ($K_1 = 0$) or to the moving porous plate ($K_1 = 1$). This concludes that in case of both the small permeable regime and pure fluid regime, Hall current tends to reduce fluid velocity in the primary flow direction and secondary flow direction in most part of the channel whereas it has reverse effect on the fluid velocity in the secondary flow direction in the vicinity of the moving porous plate. The usual nature of Hall current is to induce fluid flow in the secondary flow direction.

Figs. 6 to 9 illustrate the effect of ion-slip parameter B_i on the fluid velocity in the primary and secondary flow directions. Figs. 6 to 9 depict that in case of both the small permeable regime ($D_a = 0.01$) and pure fluid regime ($D_a \rightarrow \infty$), fluid velocity in the primary flow direction u_a^* and fluid velocity in the secondary flow direction w_a^* decrease on increasing ion-slip parameter B_i when magnetic field is either fixed relative to the fluid ($K_1 = 0$) or to the moving porous plate ($K_1 = 1$). This implies that in case of both the small permeable regime and

pure fluid regime, ion-slip tends to reduce fluid velocity in both the primary and secondary flow directions when magnetic field is either fixed relative to the fluid or to the moving porous plate.

Figs. 10 to 13 show the impact of rotation parameter K^2 on the fluid velocity in the primary and secondary flow directions. Figs. 10 to 13 represent that in case of both the small permeable regime ($D_a = 0.01$) and pure fluid regime ($D_a \rightarrow \infty$), fluid velocity in the primary flow direction u_a^* decreases whereas fluid velocity in the secondary flow direction w_a^* increases on increasing rotation parameter K^2 when magnetic field is either fixed relative to the fluid ($K_1 = 0$) or to the moving porous plate ($K_1 = 1$). This concludes that in case of both the small permeable regime and pure fluid regime, Coriolis force tends to reduce fluid velocity in the primary flow direction whereas it has reverse effect on the fluid velocity in the secondary flow direction when magnetic field is either fixed relative to the fluid or to the moving porous plate. Similar to the Hall current the usual nature of the Coriolis force is to induce fluid flow in the secondary flow direction. Our result comply it.

Figs. 14 and 15 display the effect of permeability parameter D_a on the fluid velocity in the primary and secondary flow directions. Figs. 14 and 15 show that both the fluid velocity in the primary flow direction u_a^* and fluid velocity in the secondary flow direction w_a^* increase on increasing permeability parameter D_a when magnetic field is either fixed relative to the fluid ($K_1 = 0$) or to the moving porous plate ($K_1 = 1$). This concludes that permeability of the medium tends to enhance fluid velocity in both the primary and secondary flow directions when magnetic field is either fixed relative to the fluid or to the moving porous plate.

Figs. 16 to 19 illustrate the effect of suction/injection parameter N_t ($N_t > 0$ for suction and $N_t < 0$ for injection) on the fluid velocity in the primary and secondary flow directions. Figs. 16 to 19 show that in case of both the small permeable regime ($D_a = 0.01$) and pure fluid regime ($D_a \rightarrow \infty$), fluid velocity in the primary flow direction u_a^* and fluid velocity in the secondary flow direction w_a^* increase on increasing suction parameter N_t ($\mathbf{\xi}0$) whereas

it decrease on increasing injection parameter N_t (¡0) in the lower half of the channel when magnetic field is either fixed relative to the fluid ($K_1 = 0$) or to the moving porous plate ($K_1 = 1$). In the upper half of the channel this property is reversed. This implies that in case of both the small permeable regime and pure fluid regime, suction tends to enhance fluid velocity in both the primary and secondary flow directions in the lower half of the channel whereas the injection has reverse effect on it in the lower half of the channel when magnetic field is either fixed relative to the fluid or to the moving porous plate. This effect of suction/injection is reversed in the upper half of the channel.

It is also noticed from Figs. 2 to 19 that the fluid velocity when magnetic field is fixed relative to the moving porous plate is always more than the fluid velocity when magnetic field is fixed relative to the fluid.

Figs. 20 to 23 describe the effects of Hall current parameter B_e and ion-slip parameter B_i on the shear stress at the moving porous plate in primary and secondary flow directions. Figs. 20 and 22 exhibit that in case of both the small permeable regime ($D_a = 0.01$) and pure fluid regime ($D_a \to \infty$), shear stress at the moving porous plate in the primary flow direction τ_{xa}^* increases on increasing both the Hall current parameter B_e and ion-slip parameter B_i when magnetic field is either fixed relative to the fluid ($K_1 = 0$) or to the moving porous plate ($K_1 = 1$). Figs. 21 and 23 show that in case of both the small permeable regime ($D_a = 0.01$) and pure fluid regime ($D_a \to \infty$), shear stress at the moving porous plate in the secondary flow direction τ_{za}^* decreases on increasing Hall current parameter B_e and it increases on increasing ion-slip parameter B_i when magnetic field is either fixed relative to the fluid ($K_1 = 0$) or to the moving porous plate ($K_1 = 1$). This concludes that in case of both the small permeable regime and pure fluid regime, both the Hall current and ion-slip tend to enhance shear stress at the moving porous plate in the primary flow direction when magnetic field is either fixed relative to the fluid or to the moving porous plate. In case of both the small permeable regime and pure fluid regime Hall current tends to reduce shear stress at the moving porous plate in the secondary flow direction

whereas ion-slip tends to enhance shear stress at the moving porous plate in the secondary flow direction when magnetic field is either fixed relative to the fluid or to the moving porous plate.

References

[1] S. Ahmed, A. J. Chamkha, *Hartmann Newtonian radiating MHD flow for a rotating vertical porous channel immersed in a Darcian Porous Regime:An exact solution*, International Journal of Numerical Methods for Heat and Fluid Flow 24 (2014) 1454-1470.

[2] H. A. Attia, *Unsteady Couette flow with heat transfer considering ion-slip*, Turkish Journal of Physics 29 (2005) 379-388.

[3] O. A. Beg, J. L. Sim, R. Zueco, R. Bhargava, *Numerical study of magnetohydrodynamic viscous plasma flow in rotating porous media with Hall currents and inclined magnetic field influence*, Communications in Nonlinear Science and Numerical Simulation 15 (2010) 345-359.

[4] O. A. Beg, J. Zueco and H. S. Takhar, *Unsteady magnetohydrodynamic Hartmann-Couette flow and heat transfer in a Darcian channel with Hall current, ion-slip, viscous and Joule heating effects: Network numerical solutions*, Communications in Nonlinear Science and Numerical Simulation 14 (2009) 1082-1097.

[5] D. S. Chauhan and R. Agrawal, *Effects of Hall current on MHD Couette flow in a channel partially filed with a porous medium in a rotating system*, Meccanica 47 (2012) 405-421.

[6] K. R. Cramer and S. I. Pai, *Magnetofluiddynamics for Engineers and Physicists*, McGraw-Hill Book Comp. New York (1973).

[7] S. K. Ghosh, *Effects of Hall current on MHD Couette flow in a rotating system with arbitrary magnetic field*, Czechoslovak Journal of Physics 52 (2002) 51-63.

[8] S. K. Ghosh, I. Pop, *Hall effects on unsteady hydromagnetic flow in a rotating system with oscillating pressure gradient*, Inter-

national Journal of Applied Mechanics and Engineering 8 (2003) 43-56.

[9] S. K. Ghosh, I. Pop, *Hall effects on MHD plasma Couette flow in a rotating enviornment*, International Journal of Applied Mechanics and Engineering 9 (2004) 293-305.

[10] S. K. Ghosh, O. A. Beg, M. Narahari, *Hall effects on MHD flow in a rotating system with heat transfer characterstics*, Meccanica 44 (2009) 741-765.

[11] M. Guria, R. N. Jana, *Hall effects on the hydromagnetic convective flow through a rotating channel under general wall conditions*, Magnetohydrodynamics 43 (2007) 287-300.

[12] D. B. Ingham and I. Pop, *Transport Phenomena in Porous Media II*, Pergamon, Oxford (2002).

[13] R. N. Jana and N. Datta, *Hall effects on MHD Couette flow in rotating system*, Czechoslovak Journal of Physics 30 (1980) 659-667.

[14] B. K. Jha and C. A. Apere, *Combined effect of Hall and ion-slip currents on unsteady MHD Couette flows in a rotating system*, Journal of Physical Society of Japan 79 (2010) 104401(9 pages).

[15] B. K. Jha and C. A. Apere, *Time-dependent MHD Couette flow of rotating fluid with Hall and ion-slip currents*, Applied Mathematics and Mechanics 33 (2012) 399-410.

[16] T. Linga Raju and V. V. Ramana Rao, *Hall effects on temperature distribution in a rotating ionized hydromagnetic flow between parallel walls*, International Journal of Engineeering Science 31 (1993) 1073-1091.

[17] N. W. McLachlan, *Complex Variable and Operational Calculas with Technical Application*, McGraw-Hill Book Comp., New York (1973).

[18] T. Nagy and Z. Demendy, of Hall currents and Coriolis force on Hartmann flow under general wall conditions, Acta Mechanica 113 (1995) 77-91.

[19] P. C. Ram, A. Singh and H. S. Takhar, *Effects of Hall and ion-slip currents on convective flow in rotating fluid with wall temperature oscillations*, Journal of Magnetohydrodynamics and Plasma Research 5 (1995) 1-16.

[20] H. Sato, *The Hall effect in the viscous flow of ionized gas between parallel plates under transverse magnetic field*, Journal of Physical Society of Japan 16 (1961) 1427-1433.

[21] G. S. Seth and Md. S. Ansari, *Magnetohydrodynamic Convective Flow in a Rotating Channel with Hall Effects*, International Journal of Theoretical and Applied Mechanics 4 (2009) 205-222.

[22] G. S. Seth and S. K. Ghosh, *Effet of Hall current on unsteady hydromagnetic flow in a rotating channel with oscillating pressure gradient*, Indian Journal of Pure and Applied Mathmatics 17 (1986) 819-826.

[23] G. S. Seth and J. K. Singh, *Effects of Hall current on unsteady MHD Couette flow of class-II in a rotating system*, Journal of Applied Fluid Mechcanics 6 (2013) 473-484.

[24] G. S. Seth, P. K. Mandal and R. Sharma, *Hydromagnetic Couette flow of class-II and heat transfer through a porous medium in a rotating system with Hall effects*, Journal of Mathematical Modeling 3 (2015) 49-75.

[25] G. S. Seth, J. K. Singh and G. K. Mahato, *Effects of Hall current and rotation on unsteady hydromagnetic Couette flow within a porous channel*, International Journal of Applied Mechanics 4 (2012) 1250015(25 pages).

[26] K. D. Singh, B. P. Garg and A. K. Bansal, *Hall current effect on visco-elastic MHD oscillatory convective flow through a porous medium in a vertical channel with heat radiation*, Proccedings of the Indian National Science Academy 80 (2014) 333-343.

[27] K. D. Singh and R. Kumar, *Combined effects of Hall current and rotation on free convection MHD flow in a porous channel*, Indian Journal of Pure and Applied Physics 47 (2009) 617-623.

[28] K. D. Singh and R. Pathak, *Effect of rotation and Hall current on mixed convection MHD flow through a porous medium filled in a vertical channel in presence of thermal radiation*, Indian Journal of Pure and Applied Physics 50 (2012) 77-85.

[29] R. Sivaprasad, D. R. V. Prasad Rao and D. V. Krishna, *Hall effects on unsteady free and forced convection flow in a porous rotating channel*, Indian Journal of Pure and Applied Mathematics 19 (1988) 688-696.

[30] V. M. Soundalgekar, N. V. Vighnesam and H. S. Takhar, *Hall and ion-slip effects in MHD Couette flow with heat transfer*, IEEE Transections of Plasma Science 7 (1979) 178-182.

[31] P. Sulochana, *Hall effects on unsteady MHD three dimensional flow through a porous medium in a rotating parallel plate channel with effect of inclined magnetic field*, American Journal of Computational Mathematics 4 (2014) 396-405.

[32] G. W. Sutton and A. Sherman, *Engineering Magnetohydrodynamics*, McGraw-Hill Book Comp., New York (1965).

[33] H. S. Takhar and B. K. Jha, *Effects of Hall and ion-slip currents on MHD flow past an impulsively started plate in a rotating systems*, Journal of Magnetohydrodynamics and Plasma Research 8 (1998) 61-72.

number of research papers in international journals of repute. His research areas are Fluid Mechanics, MHD and Numerical Analysis.

S. G. Begum is doing research work leading to the Ph. D. degree in Department of Studies in Mathematics, V. S. K. University, Ballari, INDIA. She has awarded Maulana Azad National Fellowship (MANF) of University Grant Commission (UGC), New Delhi in the year 2015 to carry-out research work leading to the Ph.D. degree. She has received her M.Sc. degree in Mathematics from Gulbarga University, Gulbarga, INDIA in the year 2011. She has published research papers in journals of national and international repute. Her research areas are Fluid Mechanics, MHD, Rotating Fluids and Numerical Analysis.

N. Joshi is doing research work leading to the Ph. D. degree in Department of Studies in Mathematics, V. S. K. University, Ballari, INDIA. He has received his M.Sc. degree in Mathematics from same university in the year 2012. He has published research papers in journals of national and international repute. His research areas are Fluid Mechanics, MHD Channel and Duct Flows and Numerical Analysis.

J. K. Singh is Assistant Professor in Department of Studies in Mathematics, V. S. K. University, Ballari, INDIA. He has received his Ph.D. degree in Applied Mathematics from Indian School of Mines, Dhanbad, INDIA in the year 2012. He has qualified National Eligibility Test (NET) in the years 2008 and 2009, and awarded Junior Research Fellowship (JRF) of University Grant Commission (UGC), New Delhi and Council of Scientific and Industrial Research (CSIR), New Delhi to carry-out research work leading to the Ph.D. degree. He has published a